JOURNAL OF GEOPHYSICAL RESEARCH, VOL. 103, NO. C5, PAGES 10,419–10,435, MAY 15, 1998

Retreat of the cold halocline layer in the Arctic Ocean

Michael Steele

Polar Science Center, Applied Physics Laboratory, University of Washington, Seattle

Timothy Boyd

College of Oceanic and Atmospheric Sciences, Oregon State University, Corvallis

Abstract. We present a comparison of Arctic Ocean hydrographic data sets from the 1990s, with a focus on changes in the upper few hundred meters of the Eurasian Basin. The most recent observations discussed here were collected during the spring 1995 Scientific Ice Expedition (SCICEX'95), the second in a series of scientific cruises to the Arctic Ocean aboard U.S. Navy nuclear submarines. Although the 1990s have seen an abundance of synoptic cruises to the Arctic, this was the only one to take place in winter/spring conditions. Other data considered here were collected during the first SCICEX cruise in summer 1993 (SCICEX'93) and during an icebreaker cruise to the Eurasian Basin in summer 1991 (*Oden*'91). A new Russian-American winter climatology is also used as a reference. These comparisons reveal that the Eurasian Basin "cold halocline layer" has retreated during the 1990s to cover significantly less area than in previous years. Specifically, we find a retreat from the Amundsen Basin back into the Makarov Basin; the latter is the only region with a true cold halocline layer during SCICEX'95. Changes are also seen in other halocline types and in the Atlantic Water layer heat content and depth. Since the cold halocline layer insulates the surface layer (and thus the overlying sea ice) from the heat contained in the Atlantic Water layer, this should have profound effects on the surface energy and mass balance of sea ice in this region. Using a simple mixing model, we calculate maximum ice-ocean heat fluxes of 1–3 W m^{-2} in the Eurasian Basin, where during SCICEX'95 the surface layer lay in direct contact with the underlying Atlantic Water layer. The overall cause of water mass changes in the 1990s might have been a shift in the atmospheric wind forcing and resulting sea ice motion during the late 1980s, which we speculate influenced the location where fresh shelf waters flow into the deeper basins of the Arctic Ocean. Finally, we discuss two different mechanisms that have been proposed for cold halocline water formation, and we propose a compromise that best fits these data.

1. Introduction

How much of the Arctic Ocean is covered by a cold halocline layer (CHL)? The answer is critical to studies of the sea ice mass balance, since this layer insulates the ice pack from the heat that lies at depth throughout the Arctic Ocean [*Aagaard et al.*, 1981; *Steele et al.*, 1995; M.G. McPhee, unpublished manuscript, 1980]. Figure 1 shows data collected in the Makarov Basin in 1995, where the cold, salty halocline layer above 117 m depth separates the cold, fresh surface layer from the warmer, saltier Atlantic Water (AW). Mixing in the surface layer entrains cold, near-freezing waters from below the pycnocline (which is essentially coincident with the halocline at these cold temperatures) and so has little impact on the surface heat budget. If this layer were absent, however, heat from the AW might rise to the surface, where even a few watts per meter squared can melt substantial amounts of ice [*Maykut and Untersteiner*, 1971].

The CHL represents a transition between two core water masses: cold, fresh surface waters and cold, salty Lower Halocline Water (LHW). The low-salinity surface layer derives from river and Bering Strait inflows [*Aagaard et al.*, 1981; *Steele et al.*, 1996]. The origins of LHW are still uncertain. Its formation has been ascribed to ice growth on the continental shelves of the Amundsen and Nansen Basins (collectively, the "Eurasian Basin") [*Aagaard et al.*, 1981; *Martin and Cavalieri*, 1989] as well as to air-ice-ocean exchange processes at the marginal ice zone (MIZ) of the North Atlantic [*Steele et al.*, 1995]. The concept in these schemes is that the CHL forms as cold, salty LHW from the periphery of the Arctic Ocean advects toward the deep basins, interleaving at the appropriate depth (about 100 m) into a "preexisting condition" in which a fresh, cold surface layer overlies a relatively warm, salty AW layer. This is illustrated in Figure 2a, where "upstream" and "downstream" are relative to the location along the AW inflow path where a CHL first appears (i.e., where both a fresh surface layer and saltier LHW first appear together). A very different mechanism was recently proposed by *Rudels et al.* [1996], in which the preexisting condition is a cold, salty, and deep (~100 m) convective winter mixed layer with LHW properties, and it is relatively fresh shelf waters that advect into the surface and near-surface layers (Figure 2b). In regions where these shelf waters have intruded, the deep winter layer becomes isolated from the surface; subsequent convection is presumed to be much shallower. Thus the main difference between the two CHL mechanisms is the origin of LHW waters at around 100 m depth; one is advective (Figure 2a) while the other is convective (Figure 2b). Both are winter processes.

Paper number 98JC00580.
0148-0227/98/98JC-00580$09.00

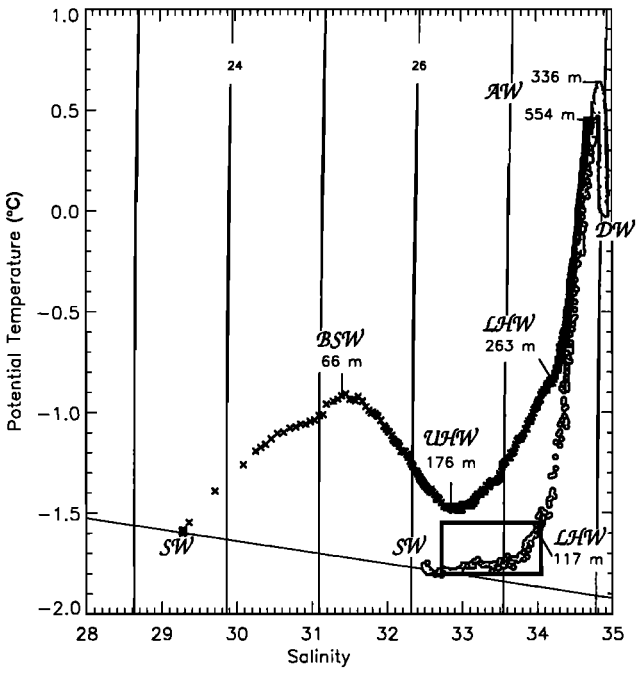

Figure 1. Potential temperature-salinity plots using data collected during the spring 1995 Scientific Ice Expedition (SCICEX'95) from the Makarov Basin (circles) and from the Canada Basin (crosses). Surface waters in both basins lie on the freezing line. The temperature maxima represent Atlantic Water; above these maxima and below the surface waters lie halocline waters of various origins. The cold halocline layer in the Makarov Basin is identified by a box; it is where salinity increases from the surface values while the temperature remains close to the freezing line.

Where a CHL exists, upward heat flux from the AW to the surface is minimal. *Steele and Morison* [1993] show an example from just north of the Barents Sea continental shelf, where ice melt and heat fluxes were nil until the camp drifted southward onto the continental shelf and the CHL disappeared. In the Canada Basin, Bering Sea Water (BSW) that lies just below the mixed layer contains some heat that is potentially available for entrainment (Figure 1). *Morison and Smith* [1981] calculated an average ice-ocean heat flux from this layer of 0.3 W m^{-2} near Ellesmere Island, far removed from Bering Strait. At locations closer to its source we find warmer BSW [*Coachman and Barnes*, 1961] and thus perhaps higher heat fluxes. In fact, these have been observed in coupled ice-ocean model results [*Zhang et al.*, 1998]. Thus the Canada Basin has what might be termed a "cool halocline" layer.

The identification of a CHL is easiest using data collected during winter, for two reasons. First, as described above, CHL formation is a winter phenomenon. Thus its properties are most distinct at this time, and the possibility exists of tracing it to its source [e.g., *Steele et al.*, 1995]. Second, in summer a fresh meltwater layer forms that by definition creates a halocline at its base. This is a seasonal phenomenon that plays little role in insulating the surface layer from relatively warm AW. Below the summer meltwater layer lies a remnant winter mixed layer, which can be distinct when deep mixing is nil [*Rudels et al.*, 1996, Figure 3a] or ambiguous [*Rudels et al.*, 1996, Figure 3b] if mixing from internal waves and/or tides creates a gradient which looks similar to the year-round pycnocline that lies below the winter mixed layer [*Padman and Dillon*, 1991; *D'Asaro and Morison*, 1992]. Although they are very different, the distinction between seasonal and year-round CHLs has not been made clear in the literature to date.

The 1990s have marked a watershed in the acquisition of Arctic Ocean hydrographic data. Much can and has been learned from these data concerning the distribution of water masses and ocean circulation. We discuss some of these data below. However, all except one of these major cruises has occurred in the summer or early fall, when transit through sea ice is easiest. The exception was the April–May cruise of the U.S. Navy submarine *Cavalla* during the Scientific Ice Expedition of 1995 (SCICEX'95). Data collected during this cruise have proven to be particularly valuable as a synoptic sample of the Arctic Ocean during spring.

Recent work has indicated that large-scale changes have occurred in the extent and strength of AW and certain halocline types during the 1990s relative to previous years [*McLaughlin et al.*, 1996; *Morison et al.*, 1998]. Here we consider what changes have occurred in the CHL. We use data collected during SCICEX'95 to examine the extent and character of the CHL in the Eurasian Basin. We also briefly consider the extent of other halocline types. Then we compare these data to those collected 2 years previously during SCICEX'93 and those collected 2 years previous to that during the 1991 cruise of the icebreaker *Oden* (*Oden*'91). We also consider what the published climatologies have to say about the CHL. For this purpose we use a newly published Russian-American Arctic climatology by the *Environmental Working Group (EWG)* [1997] (available as http://ns.noaa. gov/atlas).

A brief summary of the data sets used here is given in the following section. We then discuss the SCICEX'95 data in some detail, after which a comparison with older data from the 1990s is presented. A simple model calculation of ice-ocean heat fluxes during

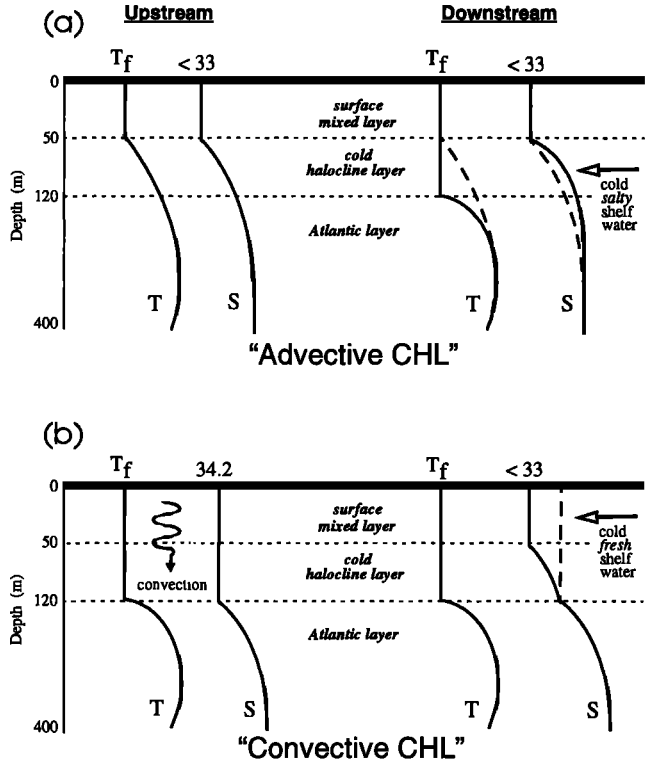

Figure 2. A schematic illustration of two mechanisms for the formation of the cold halocline layer (CHL). (a) The "advective CHL" forms by the injection into the deep basins of cold salty shelf water between a fresh surface layer and a saltier deep Atlantic layer. (b) The "convective CHL" forms by winter convection in the surface mixed layer, which is then capped by cold fresh shelf water. "Upstream" conditions are shown as dashed lines in the "downstream" schematics.

SCICEX'95 is then described. This is followed by our speculation as to the source of changes observed during the decade of the 1990s, and then followed by conclusions.

2. Methods

Three data sets and one climatology are described here: SCICEX'95, SCICEX'93, *Oden*'91, and the EWG climatology. We focus on temperature and salinity depth profiles in each case.

The EWG climatology is described by the *EWG* [1997]. Mean fields of temperature and salinity are provided on a 50 km grid over the Arctic Ocean and come from various hydrographic measurements collected during the years 1950–1989 over the winter season (December–May). The *EWG* [1997] CD-ROM provides a choice of four different grid interpolation methods; we use here the Spectral Objective Analysis method. In this study the decadal mean and 40 year mean fields of temperature and salinity are used. We also use the maximum salinity field, computed as the maximum value ever recorded over the 40 year record at each grid point and each depth.

Oden'91 was an historic first scientific icebreaker cruise across the Eurasian Basin in August–October 1991. Results have been described in a number of publications [*Anderson et al.*, 1994; *Bauch et al.*, 1995]. SCICEX'93 took place in August–September 1993 and was also historic: it was the first scientific cruise aboard a U.S.

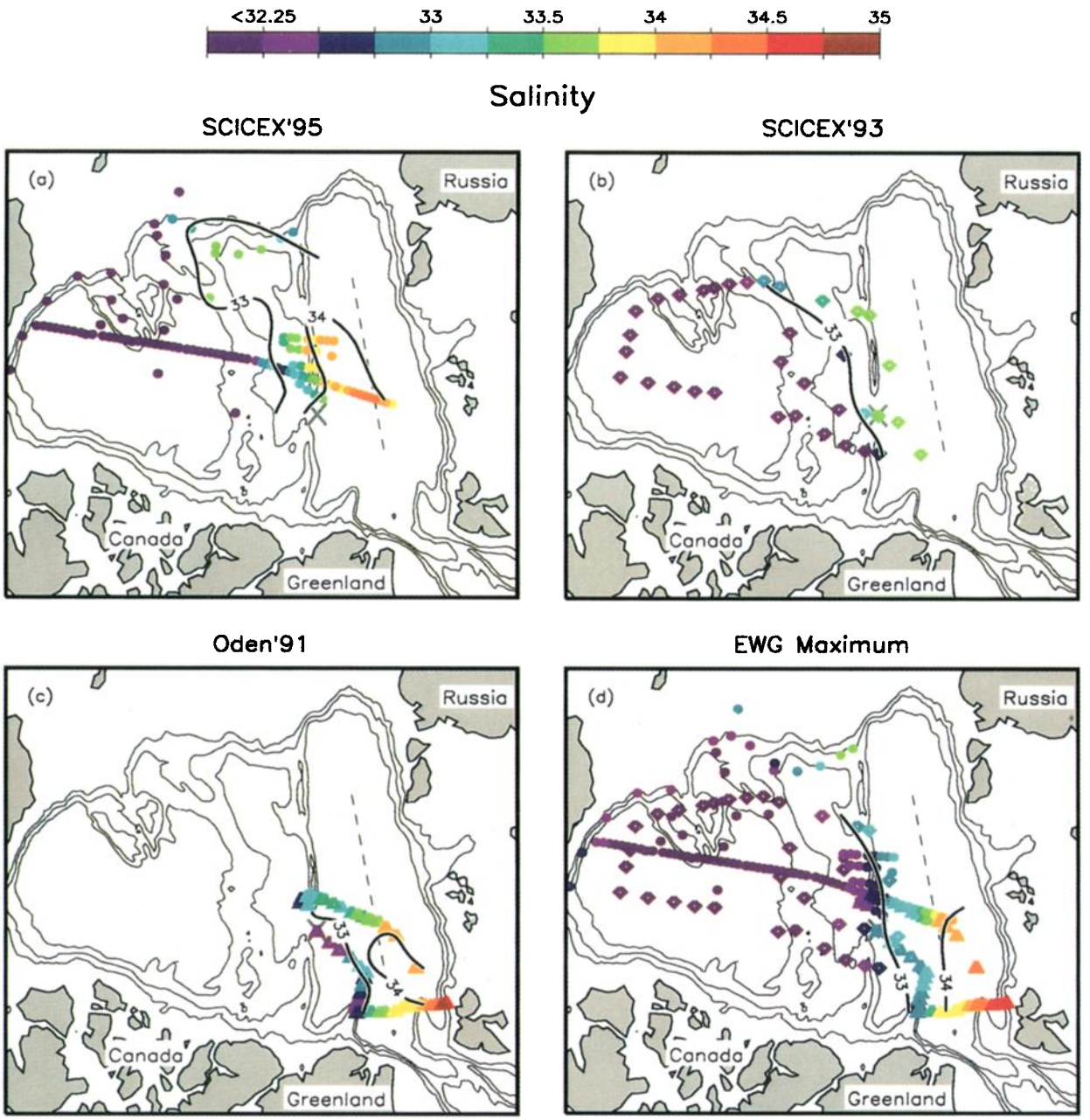

Plate 1. Mean salinity in the interval 40–60 m for (a) SCICEX'95, (b) SCICEX'93, and (c) *Oden*'91. A cross at the north pole is aligned along east longitudes 0°–180° and 90°–270°. Also shown are (d) 40 year (1950–1989) maximum salinities from the Environmental Working Group (*EWG*) [1997] winter climatology interpolated onto the station locations from the three cruises (see text for further details). We see a retreat of fresh surface waters and the cold halocline layer from the Eurasian Basin (and especially from the Amundsen Basin) during the 1990s.

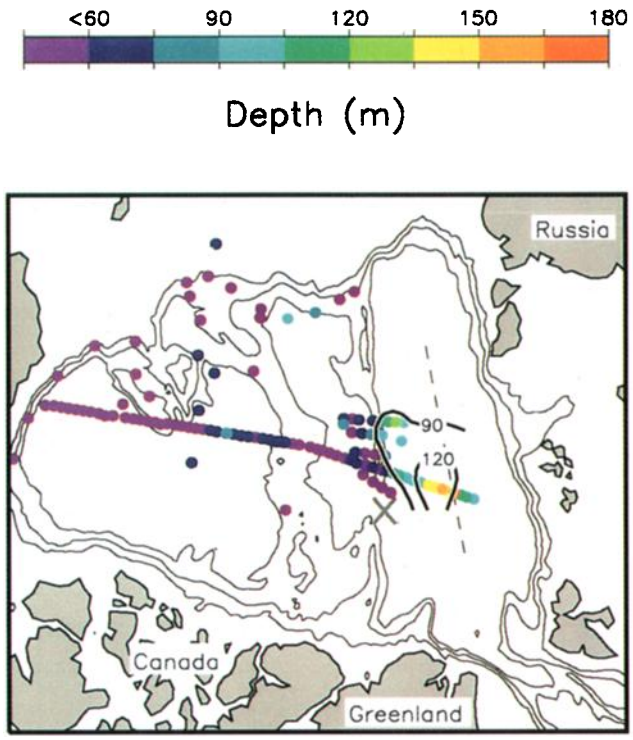

Plate 2. Mixed layer depth (in meters) during SCICEX'95 as measured by the depth where salinity increases from the uppermost recorded value by 0.1. The deepest mixed layer lies near the Nansen-Gakkel Ridge, where the influence of freshwater sources from rivers and the seasonal sea ice melt zone is weakest.

Navy nuclear submarine to the Arctic Ocean. Results are described by *Morison et al.* [1998].

SCICEX'95 was conducted in April–May 1995. A variety of physical and chemical observations were taken. Here we focus on temperature and salinity profiles obtained while the ship was under way using expendable conductivity-temperature-depth profilers (XCTDs) manufactured by Sippican. *Morison et al.* [1998] describe the instrument and its deployment. The uppermost part of the water column is not sampled by the XCTDs and also contains some thermal lag errors that develop during deployment. The shallowest depth with good data during SCICEX'95 ranged from 19 to 42 m, with a mean of 29 m.

Calibration of XCTD data was accomplished by comparing with five "surface casts" made by bringing the submarine up through the sea ice and deploying a SeaBird SBE-19 conductivity-temperature-depth profiler (CTD) through the ice using a portable winch. Postcruise calibration of this CTD revealed a temperature drift of 0.001°C and a salinity drift of 0.01. (The latter was partly a result of a crack in the conductivity cell that developed some time during the cruise.)

Errors in the XCTD temperature and salinity data can be thought of as resulting from two separate sources: sensor errors and depth errors. Sensor error was determined by comparison of XCTD and CTD casts in a region of low variability (a 100 m depth layer below the thermocline). Average temperature sensor errors were 0.02°C with a standard deviation of 0.013°C, and the average salinity error was 0.014 with a standard deviation of 0.007.

A last-minute change in the tail assembly of the XCTD created a fall rate uncertainty as well. This led to a depth uncertainty in these data of about 10%; i.e., about 5 m at 50 m depth and about 50 m at 500 m depth. Because of pressure dependence of conductivity this results in an additional salinity error of 0.002 at 50 m, increasing to 0.03 at 500 m. The depth error also results in a small potential temperature error of 0.004°C at 500 m.

Combining the CTD drift and XCTD sensor and depth errors results in estimated salinity errors that range from 0.03 at 50 m to 0.06 at 500 m. Potential temperature errors range from 0.03°C at 50 m to 0.04°C at 500 m. These uncertainties do not impact the analyses we present below, which depend on *T-S* properties with precisions on the order of 0.1. (Preliminary analysis of data from subsequent cruises indicates that the fall rate error of newer XCTD models has been considerably reduced (M. Moustafa, Science Applications International Corporation, personal communication, 1997).)

3. SCICEX'95 Data

Figure 3 shows station locations for SCICEX'95 (dots), SCICEX'93 (diamonds), and *Oden*'91 (triangles). Together, these cruises covered much of the interior Arctic Ocean. Gaps remain near Canada and Greenland, the Russian continental shelves, and the eastern Eurasian Basin. This last region was recently surveyed by R/V *Polarstern* in 1996; future comparisons with the data shown in Figure 3 should prove illuminating. A fortuitous overlap in ship tracks exists between SCICEX'95 and *Oden*'91 in the mid-Eurasian Basin. Selected bathymetric contours show the major basins and ridges; the Nansen-Gakkel Ridge is quite deep in most places (sill depth generally around 3500 m) and is schematically illustrated by a dashed line.

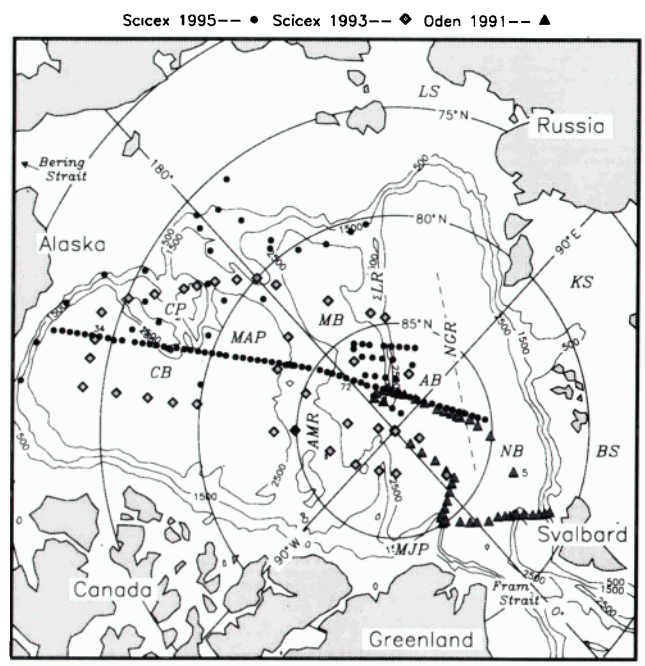

Figure 3. Stations where temperature and salinity depth profiles were taken during SCICEX'95 (dots), SCICEX'93 (diamonds), and *Oden*'91 (triangles). SCICEX'95 stations 34 and 72 (used in Figure 1) and *Oden*'91 station 5 (used in Figure 6) are marked. The 500, 1500, and 2500 m isobaths are shown; the Nansen-Gakkel Ridge (NGR) is quite deep and is thus shown schematically by a dashed line. Also shown are the following geographic place names mentioned in the text: Canada Basin (CB), Mendeleyev Abyssal Plain (MAP), Makarov Basin (MB), Amundsen Basin (AB), Nansen Basin (NB), Laptev Sea (LS), Kara Sea (KS), and Barents Sea (BS). Also shown are the Chukchi Plateau (CP), Alpha-Mendeleyev Ridge (AMR), Lomonosov Ridge (LR), and Morris-Jessup Plateau (MJP).

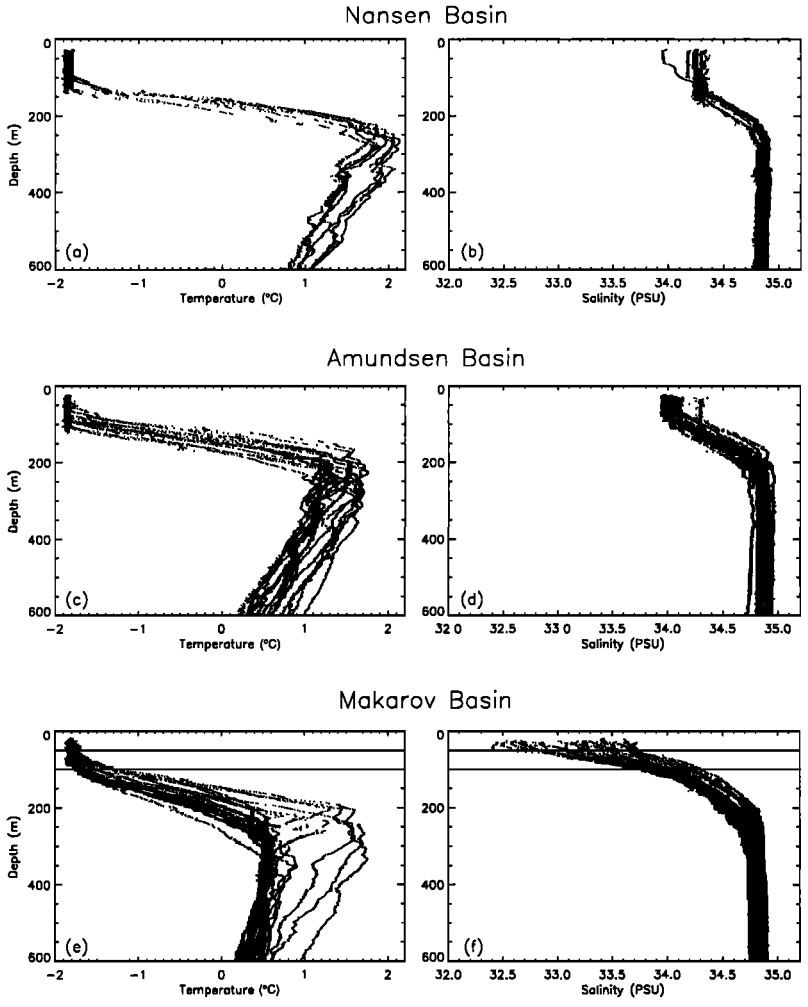

Figure 4. Temperature and salinity profiles obtained during SCICEX'95 from the (a, b) Nansen Basin, (c, d) Amundsen Basin, and (e, f) Makarov Basin. A cold halocline layer is absent from the Nansen and Amundsen Basins but is present in the Makarov Basin roughly between 50 and 100 m depth. The mixed layer is saltiest and deepest over the Nansen-Gakkel Ridge (included in Figures 4a and 4b). Atlantic Water is warmest in the Nansen Basin, slightly cooler in the Amundsen Basin, and markedly cooler in the Makarov Basin. A transition region over the Lomonosov Ridge (included in Figures 4e and 4f) about 100 km wide shows a combination of Amundsen and Makarov Basin hydrographic properties.

3.1. Temperature and Salinity Profiles

We first consider only the data from SCICEX'95. Figure 4 shows temperature and salinity profiles from the three basins of the eastern Arctic. The Nansen Basin (Figures 4a and 4b) includes data from over the Nansen-Gakkel Ridge.

The Nansen and Amundsen Basins (Figures 4a–4d) do not exhibit a CHL; that is, temperature and salinity in the surface layer are uniform down to the same depth. This layer is quite deep in places, up to about 150 m over the Nansen-Gakkel Ridge, where it is also the most saline surface layer in the data set, averaging about 34.25. It is shallower and fresher both north and south of the Nansen-Gakkel Ridge, although the data coverage to the south is limited. With regard to AW, core temperatures are highest in the Nansen Basin and slightly cooler in the Amundsen Basin.

The Makarov Basin data (Figures 4e and 4f) show a much cooler AW and a definite CHL in the 50–100 m depth range. A transition region exists in the Makarov Basin (Figures 4e and 4f) within about 100 km of the Lomonosov Ridge, where the deep AW is as warm as the Amundsen Basin, but the surface waters are fresh like the rest of the Makarov Basin. The presence of this transition region demonstrates how nominally vertical fronts are in fact tilted horizontally; that is, fronts in the halocline layers are not necessarily coincident with fronts in the AW. This point was also made by *McLaughlin et al.* [1996] with regard to fronts in the Canada Basin.

The Makarov Basin data do not show the presence of either BSW (which would appear as a temperature maximum at salinities of 31–32) or Upper Halocline Water (UHW), which is marked by a temperature minimum several tenths of a degree above freezing at a salinity of 33.1 (Figure 1). Thus the Makarov Basin shows no influence from Pacific Ocean water masses in the SCICEX'95 data, a situation observed during SCICEX'93 as well [*Morison et al.*, 1998]. Note, however, that Pacific influence can be detected in chemical tracer data (which are unfortunately unavailable from the Eurasian Basin in SCICEX'95) when it is absent in the corresponding hydrographic data [*Moore et al.*, 1983].

3.2. Temperature-Salinity Plots

The *T-S* plots for the three basins are presented in Figure 5. Again, the two obvious trends are the cooling of AW and the presence of a CHL only in the Makarov Basin. Data from the Nansen

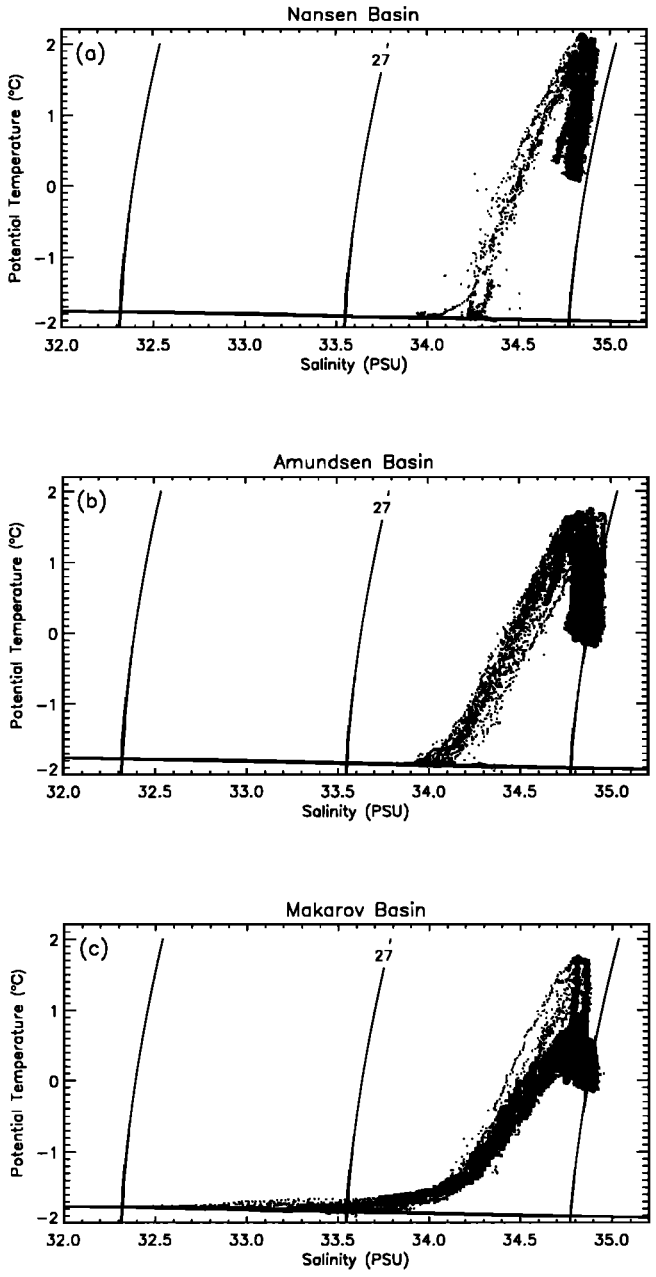

Figure 5. Potential temperature-salinity plots corresponding to Figure 4. The absence of a cold halocline layer (CHL) in (a) the Nansen Basin and (b) the Amundsen Basin is striking, where high surface salinities of about 34.0–34.2 are consistent with active formation of Lower Halocline Water. It is only in (c) the Makarov Basin where surface (and subsurface) salinities decrease enough to form a true CHL.

and Amundsen Basins have a nearly linear slope between the relatively salty surface layer and warm AW. In particular, data from over the Nansen-Gakkel Ridge show a surface mixed layer at freezing temperatures and a salinity of about 34.25, i.e., core hydrographic properties of LHW [*Jones and Anderson*, 1986]. Other data from either side of the Nansen-Gakkel Ridge show a very slight upward concavity in the thermocline and a slightly fresher surface layer of about 34.0.

What would Figures 5a and 5b look like if the data were obtained during the following summer? The answer is that the fresh summer melt layer should extend the *T-S* data toward the left, close to or just above the freezing line. An example is shown in Figure 6, which presents temperature and salinity data from *Oden*'91 station 5 in the Nansen Basin (also shown by *Rudels et al.* [1996, Figures 3 and 5]; location marked in our Figure 3). The profiles in Figure 6 show a distinct summer melt layer of about 30 m depth overlying an equally distinct remnant winter mixed layer that extends down to about 130 m with a salinity of about 34.2. The θ-*S* curve in Figure 6 looks something like the SCICEX'95 data from the Makarov Basin (Figure 5c). However, the surface salinity is higher in Figure 6 (about 33.5) relative to those in Figure 5c (about 33.0). The clear remnant winter mixed layer indicates that ice growth in this region probably erases the summer melt layer. A simple calculation reveals that about 0.6 m of growth would be sufficient; this is an upper bound since we have not accounted for the positive feedback from convection-generated upward salt flux.

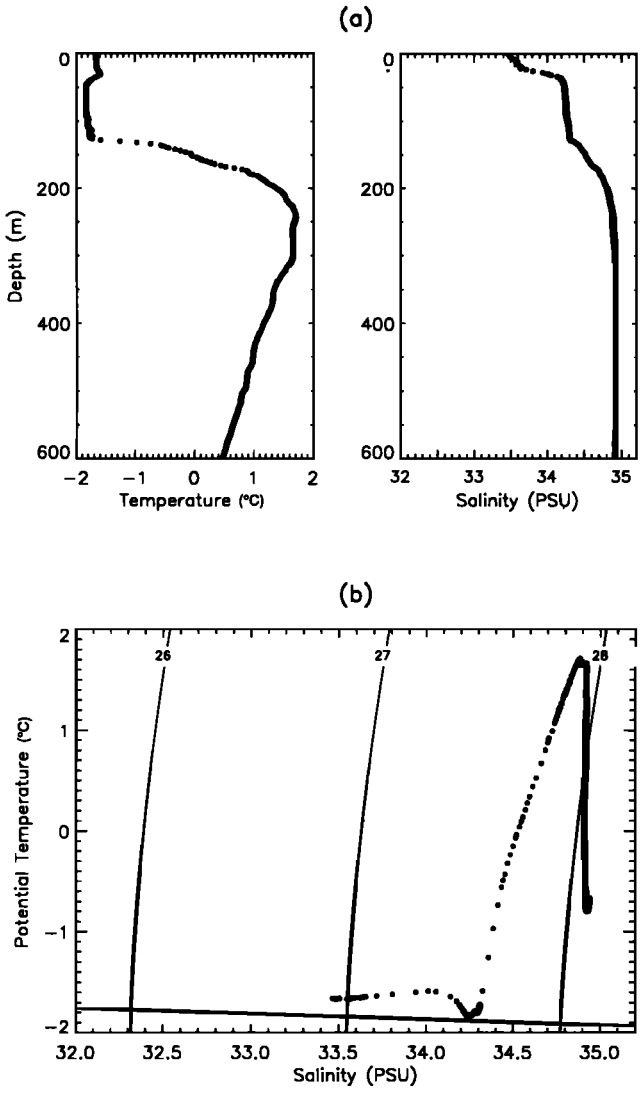

Figure 6. Station 5 from *Oden*'91 in the Nansen Basin. (a) Typical summer conditions wherein a shallow (30 m thick) fresh ice meltwater layer overlies a deeper remnant winter mixed layer that extends down to about 130 m depth. (b) The corresponding θ-*S* plot shows a hint of what might be termed a cold halocline layer (CHL) that results from stratification between the summer and winter mixed layers. We refer to this as a "seasonal CHL."

Therefore the meltwater layer shown in Figure 6 most likely does not provide year-round insulation of the surface waters from the AW heat and thus might be termed a "seasonal CHL."

The *T-S* plots in Figure 5 are highly reminiscent of the schematic plots in work by *Rudels et al.* [1996, Figure 17], which were used to illustrate their proposed mechanism for the formation of a CHL. We briefly restate their mechanism here in the context of our Figure 5. As inflowing waters from the North Atlantic encounter sea ice in eastern Fram Strait, a surface melt layer is created. In winter this melt layer "wedge" [*Untersteiner*, 1988] eventually gives way, downstream, to a deep mixed layer forced by surface convection from freezing sea ice. At this point the upper ocean should look something like Figures 4a, 4b, and 5a. Farther downstream, along the continental shelf break of the Nansen Basin, seasonal transitions occur which do not substantially modify the annual mean upper ocean structure. Thus the Nansen Basin (at least over the inflowing AW core) has no year-round CHL. The next major modification occurs when relatively fresh riverine waters from the Kara and Laptev Seas ("shelf waters" in *Rudels et al.* [1996] terminology) are injected into the surface and near-surface waters. This "caps" the LHW by bringing the (annual average) surface salinities down and, with some subsurface injection, "lifts" the *T-S* curve off the freezing line above the 34.25 core salinity of LHW. It is this riverine source water that provides, in the *Rudels et al.* [1996] scheme, the necessary surface stratification for a year-round CHL.

An important point for our purposes is that using data collected up through the summer of 1991, *Rudels et al.* [1996] found a riverine influence in the Amundsen Basin. That is, they noted the presence of relatively fresh surface waters and a CHL in the Amundsen Basin. A comparison with our Figures 4c, 4d, and 5b shows that conditions had changed significantly by the time of SCICEX'95. This change is explored further in the next section.

4. Comparison with Previous Data

4.1. Retreat of the Cold Halocline Layer

Plate 1a shows the spatial variations of the mean salinity from SCICEX'95 over the depth interval 40–60 m. This represents the winter mixed layer salinity in much of the data (particularly the Eurasian Basin), although some profiles are stratified to shallower depths and some to the uppermost readings at 20–30 m. We use this depth interval in order to compare with the SCICEX'93 and *Oden*'91 data sets, which contain a shallow summer melt layer. (Maximum mixed layer depths in these summer cruises was about 40–45 m and were most frequently much shallower.) We also use this salinity as a tracer for the presence or absence of a CHL. Where it is high and 34–34.25, the winter mixed layer shows evidence of active LHW formation, and a CHL is absent (e.g., Figures 4a, 4b, and 5a). Where it is much fresher, LHW is capped by a stable pycnocline and a CHL is present (e.g., Figures 4e, 4f, and 5c).

In Plate 1a, a sharp front at a salinity of about 34 delimits the fresh waters of the Makarov and Canada Basins from the saltier waters of the Amundsen and Nansen Basins. (Here we use a color scale designed to focus on spatial variability in the eastern Arctic. The minimum value in Plate 1a is 29.8 at a station in the Canada Basin. A few smoothed contours are also plotted on Plates 1a–1d and similar plates to follow.) Note that the sharp salinity front is roughly located over the Lomonosov Ridge but at an angle that is aligned more or less along the mean axis of sea ice outflowing from the Arctic Ocean through Fram Strait in the transpolar drift stream [*Colony and Thorndike*, 1984]. Using this front as a marker for CHL extent, we conclude that a CHL was absent from the mid-Nansen and mid-Amundsen Basins during SCICEX'95.

Plates 1b and 1c show the same type of plot as Plate 1a but using data collected during SCICEX'93 and *Oden*'91. Plate 1c shows high salinities in the very salty AW as it flows, still at a shallow depth, into the Arctic Ocean north of Svalbard. The SCICEX'95 and *Oden*'91 data sets both show high salinities of about 34 within the Nansen Basin. The Amundsen Basin is another story, however. Here a marked salinification has occurred in 1995 relative to 1991. The 1993 data, although sparse in this region, fall somewhere in between the very fresh 1991 data and the much saltier 1995 data. An examination of individual profiles from *Oden*'91 obtained in the Amundsen Basin shows the presence of a CHL [see *Rudels et al.*, 1996], while Figures 4c, 4d, and 5b demonstrate its absence in that region during SCICEX'95.

Plate 1d shows the equivalent salinities from the *EWG* [1997] winter climatology. Here we have performed a two-dimensional linear interpolation from the EWG gridded profiles onto the station locations from SCICEX'95, SCICEX'93, and *Oden*'91 and then plotted the mean salinity over 40–60 m depth. We considered two different types of three-dimensional salinity fields from the EWG data set: (1) the 40 year average (1950–1989) field and (2) the decadal maximum salinity fields, defined as the maximum value at each three-dimensional grid point over each decade. From the latter we created a 40 year maximum field, which we use in Plate 1d. (The mean field is generally not fresher than 0.25 relative to the maximum field. An exception is along the western Eurasian Basin track of *Oden*'91, where the mean field is 0.5–1.0 fresher than the maximum field.) We also created a 40 year minimum field, which is referred to below. Additionally, the EWG climatology provides fields of standard deviation within each decade. The 40 year average field of salinity standard deviation at 50 m depth is generally 0.35–0.45 within the central Arctic Ocean.

Plate 1 shows that the 1990s salinities (Plates 1a–1c) are equal to or higher than the maximum salinities ever recorded in the *EWG* [1997] 1950–1989 data set (Plate 1d) at nearly all locations resolved by the color scale. The Makarov and central Amundsen Basins have undergone the strongest salinification. Salinities in these regions recorded during SCICEX'95 (Plate 1a) are higher by about 1.0 relative to the EWG maxima (Plate 1d). We can also compare the 1990s data with the EWG 40 year mean and 40 year minimum fields, again averaged over 40–60 m depth. These comparisons (not shown) demonstrate that the western Eurasian Basin during *Oden*'91 was about equal to the 40 year mean, while much of the Canada Basin was fresher than the 40 year mean during the SCICEX cruises. In fact, the central Canada Basin exhibits a freshening of about 0.5 relative to the EWG minimum field. Thus the Canada Basin (and its outflow north of Greenland toward Fram Strait) freshened as the Eurasian Basin salinified during the past decade.

To the extent that we can rely on these data sets, Plate 1 indicates that the salinification of the central Eurasian Basin (and especially the Amundsen Basin) is unprecedented in the last 40 years. Comparison of Plates 1c and 1d suggests that changes were already under way in 1991. Recent hydrographic and meteorological analyses [*Morison et al.*, 1998; *Walsh et al.*, 1996] have indicated that these changes may have started in the late 1980s.

4.2. Retreat of the River Water Front

The *Rudels et al.* [1996] mechanism for CHL formation depends on the injection of fresh shelf waters (principally from the riverine-influenced Kara and Laptev Seas) into the surface and near-surface

layers. In the *Oden*'91 data the southern extent of this water was mapped [*Rudels et al.*, 1996] using *T-S* analysis and found to be roughly over the Nansen-Gakkel Ridge. South of this boundary, freshwater was derived not from rivers but, rather, from melting sea ice. This partition in freshwater origins is most clearly seen using oxygen isotope data [*Schlosser et al.*, 1994; *Bauch et al.*, 1995], which places the front essentially coincident with the salinity front in Plate 1c, i.e., over the Nansen-Gakkel Ridge.

Unfortunately, during SCICEX'95, only five oxygen isotope profiles were taken. More frequent samples were collected at the submarine cruising depth of 134 m, which is too deep to capture significant variation in our region of interest [*Bauch et al.*, 1995]. As noted previously, however, the riverine signal is so obviously fresh that winter mixed layer salinity is a very adequate proxy for the more rigorous oxygen isotope method. Plate 1 thus indicates that between 1991 and 1995, river water retreated back from the Amundsen Basin into the Makarov Basin.

This retreat of river waters from the Eurasian Basin creates a broad area where surface waters feel little influence from freshwater sources. That is, the riverine influence has retreated to the Makarov Basin, while the large summertime meltwater source from the seasonal sea ice zone lies some distance to the south in the Barents and Kara Seas. The result is (winter) surface salinities that far exceed climatological values (Plate 1). Logically, we find the saltiest values in Plate 1a near the center of the Eurasian Basin roughly over the Nansen-Gakkel Ridge, i.e., farthest away from the aforementioned freshwater sources. (We do not imply here any topographic control by the Nansen-Gakkel Ridge.)

Additional salinization of the surface layer in the vicinity of the Nansen-Gakkel Ridge might occur via vertical mixing and entrainment of deeper waters. Plate 2 shows the mixed layer depth during SCICEX'95, defined as the depth at which salinity increases by 0.1 relative to the surface value. (It should be kept in mind that absolute depths are uncertain to about 10% in this data set.) The deepest values are over the Nansen-Gakkel Ridge, and this does not change qualitatively when other salinity increments (e.g., 0.05 or 0.2) are used. Thus the mixed layer is deepest (Plate 2) and saltiest (Plate 1) in this region. This is consistent with a minimal influence from freshwater sources and with the presence of active mixed layer deepening and entrainment. The entrained AW presumably mixes to the surface and suppresses ice growth, a subject we explore further in section 5.

4.3. Advance of Atlantic Water Into the Arctic Ocean

The CHL retreat is associated with an advance of AW into the Arctic Ocean. Plate 3 shows the AW temperature for the three cruises discussed here. We use the 40 year mean (not maximum) *EWG* [1997] temperature and salinity fields in this and all subsequent plates. A warming of Eurasian Basin AW through the 1990s is evident. Plate 3 also shows an enhancement of (warm) AW return flow toward Greenland along the Lomonosov Ridge, at least during the SCICEX cruises. In contrast, the data provide no evidence of a similar AW return flow along the Nansen-Gakkel Ridge such as proposed by *Rudels et al.* [1994]. Instead, we see evidence of fairly uniform AW properties within the Nansen Basin, with a definite front at the Nansen-Gakkel Ridge, similar to findings by *Swift et al.* [1998]. This might imply enhanced horizontal mixing, perhaps by eddies, in the Nansen Basin. Recent high-resolution numerical experiments support this scenario (W. Maslowski, Naval Postgraduate School, personal communication, 1997).

Plate 4 shows the depth of the 0°C isotherm in the three cruises and in the *EWG* [1997] data. This isotherm is often used to define the upper limit of AW [e.g., *EWG*, 1997]. Plate 4 shows that during the 1990s the AW layer has shoaled within the Amundsen Basin (about 40 m), in addition to the warming shown in Plate 3. Comparison with EWG data (40 year mean) indicates that this shoaling had just begun during *Oden*'91. Shoaling is also evident in other regions (e.g., along the Siberian continental shelf break).

The SCICEX'95 data therefore indicate that the Nansen-Gakkel Ridge is somewhat special but not in the sense proposed by *Rudels et al.* [1994]; that is, there is no evidence of a return AW core. Instead, we see a wintertime surface salinity maximum (Plate 1) that results from a retreat in riverine water extent and perhaps also from entrainment of AW from below. How much heat is mixing to the surface by this process? And what implications does this have for the sea ice mass balance? We return to these questions in section 5.

4.4. Pacific-Influenced Water Types

Our focus in this paper is on the CHL. We here briefly consider halocline water types of Pacific Ocean origins in order to explore the extent of CHL in the western Arctic.

4.4.1. Bering Sea Water. As noted previously, the Canada Basin halocline contains at least two water masses not found in the Eurasian Basin: Bering Sea Water (BSW) and Upper Halocline Water (UHW). The former is generally above the freezing point and thus can represent a source of heat to the mixed layer and overlying sea ice. Plate 5a shows the temperature in this layer during SCICEX'95 (determined as the maximum temperature for salinities less than 33, since this salinity marks the core of underlying UHW). Stations with no salinity below 33 are not colored. BSW is warmest in the Canada Basin, cooling into the Mendeleyev Abyssal Plain. The Makarov Basin contains waters that are fresh enough to be included in this plot, but their near-freezing temperatures reveal their non-BSW character. Figure 1 shows an example from the Makarov Basin, where these fresh waters contain no discernible temperature maximum. Thus the true BSW boundary lies somewhere over the Alpha-Mendeleyev Ridge, where the temperatures in Plate 5a drop to near-freezing (marked roughly by the –1.6°C isotherm).

Comparison between Plates 5a, 5b, and 5c reveals no outstanding temporal trend during the 1990s. However, *Morison et al.* [1998] did find a shift in BSW extent in SCICEX'93 relative to climatologies, and comparison of the SCICEX data (Plates 5a and 5b) and the climatology (Plate 5d) shows a BSW warming of about 0.5°C in the Canada Basin.

Plate 5 shows that BSW warms toward Alaska and Bering Strait, a not surprising result. A transition in BSW core temperature can be seen over the Chukchi Plateau (Plate 5a), marking a cooler Mendeleyev Abyssal Plain from a warmer Canada Basin. Does warmer BSW in the Canada Basin cause enhanced heat flux into the mixed layer in this region? This is explored in section 5.

4.4.2. Upper Halocline Water. Plate 6 shows the mean potential temperature in the salinity range 33.0–33.1, the core salinity of UHW [*Jones and Anderson*, 1986]. *Coachman and Barnes* [1961] call this Bering Sea Winter Water and note that it is typically 0.2°–0.3°C above freezing. They speculate that this heat is acquired on the Arctic shelves. In any case, we see a sharp temperature front over the Alpha-Mendeleyev Ridge in Plate 6a (marked roughly by the –1.7°C isotherm), similar to that in Plate 5a. The water in this salinity range within the Makarov Basin is near or at the freezing point. Figure 1 shows an example; this is not true UHW but rather Eurasian Basin waters that have been modified by river inflows and mixing. Like the BSW, we conclude that UHW is limited by the Alpha-Mendeleyev Ridge in SCICEX'95.

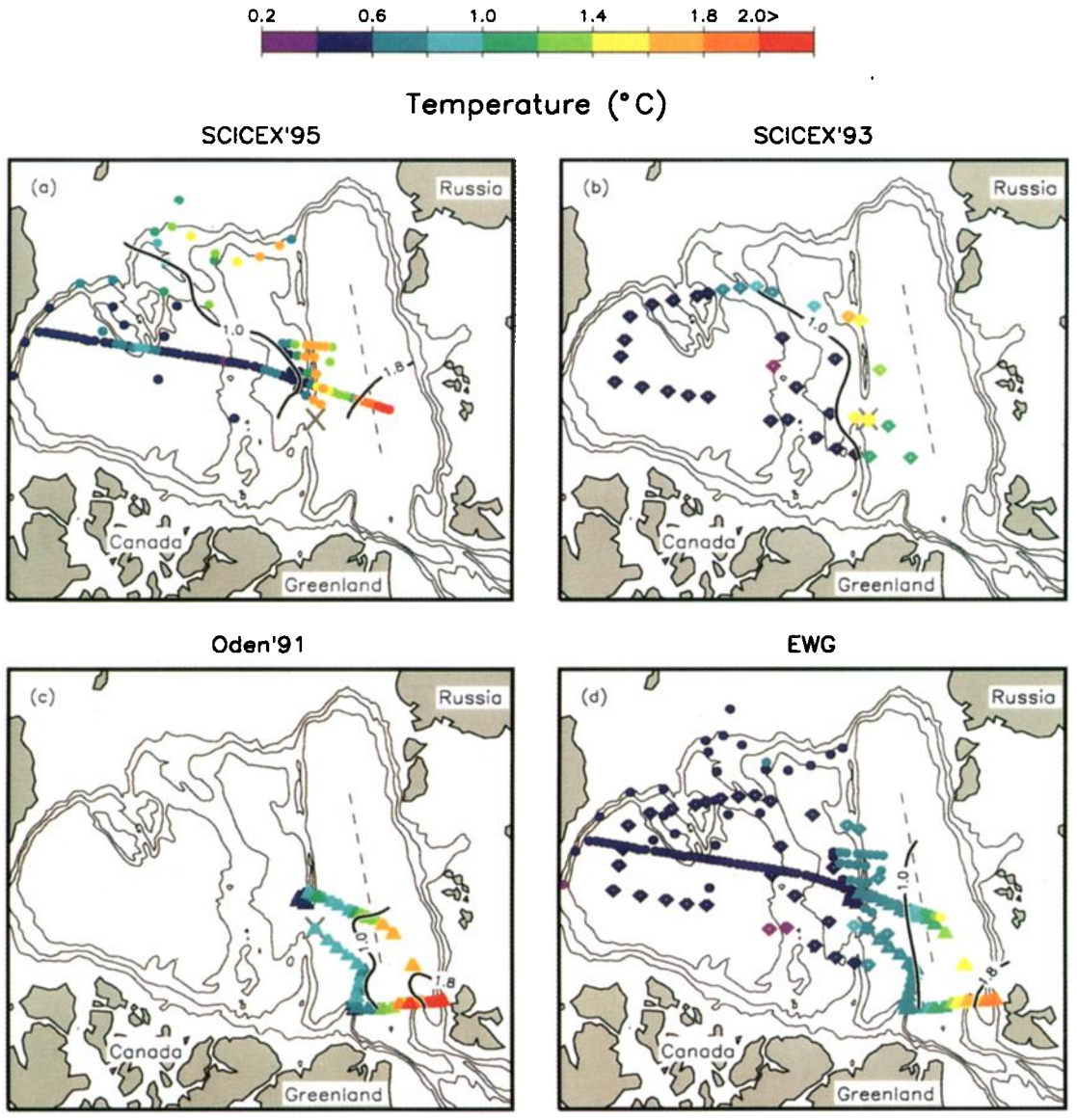

Plate 3. Same as Plate 1 but for the maximum temperature in each profile for salinities greater than 33.5. This serves as a tracer for the warm, salty Atlantic Water layer, which has warmed noticeably over the 1990s. Note the sharp front at the Nansen-Gakkel Ridge as well as the warm core over the Lomonosov Ridge in the 1990s. The *EWG* [1997] data used in this and subsequent plates is from the 40 year (1950–1989) mean fields of temperature and salinity.

Turning to the *Oden*'91 data, Plate 6c shows a slight warming in the Makarov Basin (near the north pole) relative to values in the Amundsen Basin. Although these temperatures are not nearly as high as in the Canada Basin during the SCICEX cruises, they may indicate a weak UHW presence. *Anderson et al.* [1994] found a silicate maximum in the Makarov Basin during *Oden*'91, a signature of UHW [*Jones and Anderson*, 1986]. However, they noted that their maximum values were about 3 times lower than values obtained nearby at the Lomonosov Ridge Experiment (LOREX) Ice Camp about 10 years earlier. They suggested that the UHW boundary undergoes temporal variations; the implication was that the eastern boundary might have been farther toward Europe in the years before *Oden*'91. If so, then the LOREX data and Plate 6 suggest that the UHW front has shifted from a position on the European side of the Lomonosov Ridge during the 1980s, to roughly over the ridge during *Oden*'91, and then to roughly over the Alpha-Mendeleyev Ridge during SCICEX'95. If true, then this represents yet another halocline water mass "retreat" from the Eurasian Basin.

4.4.3. A Canadian warm pool off the Morris-Jessup Plateau. We also note an interesting pool of warm water over the Morris-Jessup Plateau in Plates 5c and 6c. This pool is clearly of Canadian origins, showing evidence of a BSW temperature maximum and UHW temperatures as observed by *Coachman and Barnes* [1961]. Its probable origin in the Canada Basin was discussed by *Anderson et al.* [1994]. Dynamically, this water might be spun off a current of Canada Basin origins and properties that moves toward Fram Strait along the continental shelf break north of Greenland [*Newton and Sotirin*, 1997]. It has been proposed (R. Pawlowicz, University of British Columbia, personal communication, 1996) that such an "Arlis current" makes a sharp turn along the Morris-Jessup Plateau and in the process feeds a pool of water with Canada Basin properties just off the plateau. The *Oden*'91 data support this conjecture. Further, the strength of the Canadian influence in this region

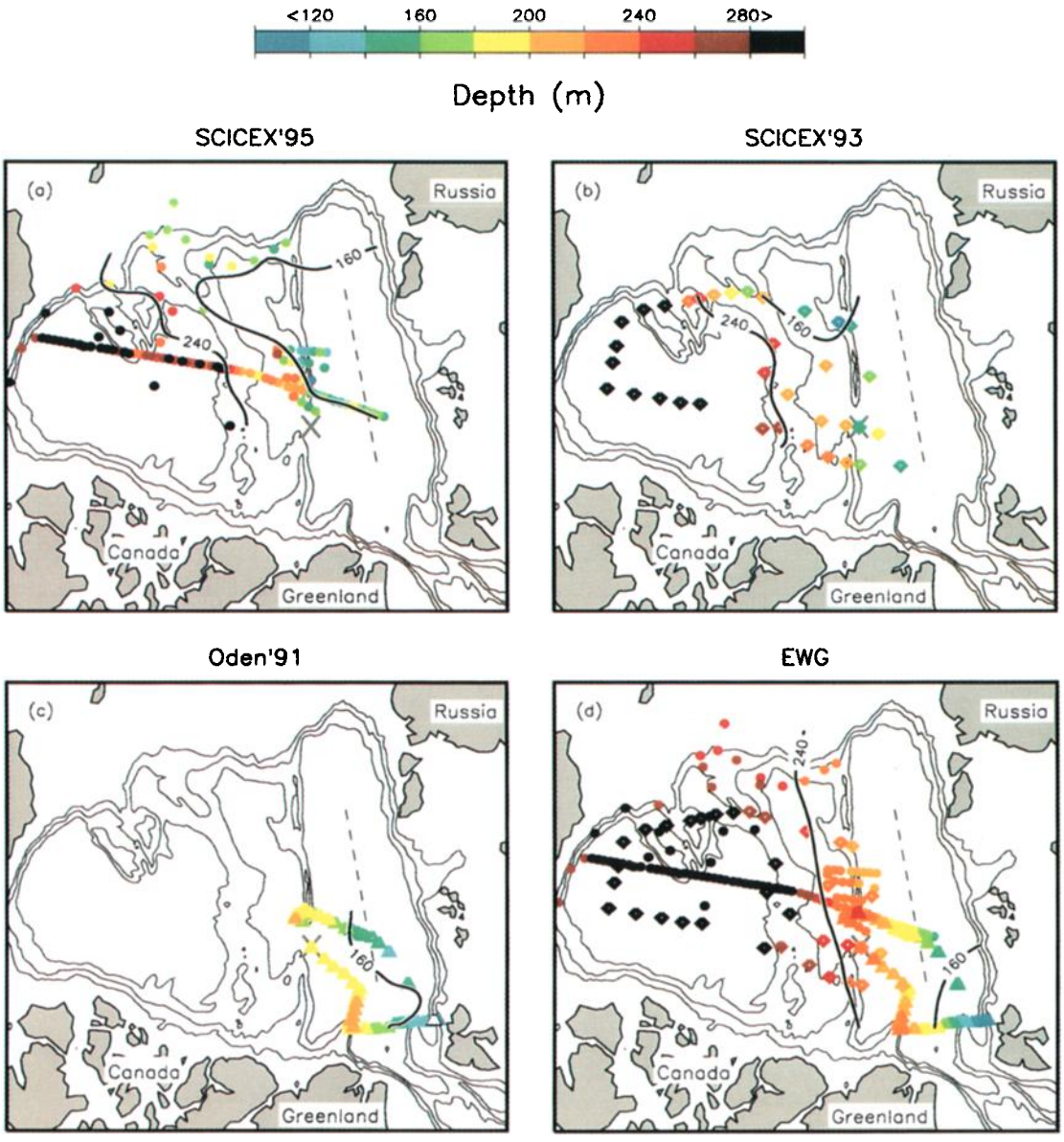

Plate 4. Same as Plate 3 but for the depth of the 0°C isotherm in each profile. This serves as a measure of the height within the water column of the upper surface of the Atlantic Water layer. We see a shoaling in the Eurasian Basin of 40–60 m during the 1990s.

is stronger than in the *EWG* [1997] climatology (Plates 5d and 6d). This might result from the increased influence of Atlantic water masses in the Russian sector of the Arctic Ocean, which could be pushing the Pacific water masses of the Canadian sector out through both the Canadian Archipelago and Fram Strait. Of course, its absence in the climatology might simply be a by-product of data resolution and/or smoothing.

5. Surface Heat Fluxes

The physical significance of the CHL is its ability to insulate the ocean surface from the heat contained in the AW. SCICEX'95 data indicate that the CHL has retreated, which means that the surface winter mixed layer now lies in direct contact with the underlying AW throughout much of the Eurasian Basin. The result should be enhanced heat fluxes and a reduction in ice growth during winter.

We explore this possibility by using a simple one-dimensional model to predict the surface heat fluxes during SCICEX'95. The model is initialized with observed temperature and salinity profiles. An assumed, idealized surface stress is then imposed that creates turbulence and mixing. The experiment is run for 20 days, and results are shown for the final time step. Where a CHL is absent or weak, upward vertical heat fluxes result.

The model is identical to that used by *Mellor et al.* [1986] and *Steele et al.* [1989]. It is a simple diffusion equation solver for temperature, salinity, and momentum, where the turbulent diffusion/viscosity coefficients are predicted using the "level 2.5" turbulence model of *Mellor and Yamada* [1982]. No sea ice model is used here; rather, the surface boundary conditions on temperature and salinity are simply fixed observed values. The surface boundary condition on momentum is a fixed stress; three different values (all climatologically "reasonable") are used. Bottom boundary conditions at 450 m are also fixed at the observed values for temperature and salinity and are zero for momentum.

The result is shown in Plate 7, where the surface stress τ is fixed at a climatologically average value [e.g., *McPhee*, 1992] of

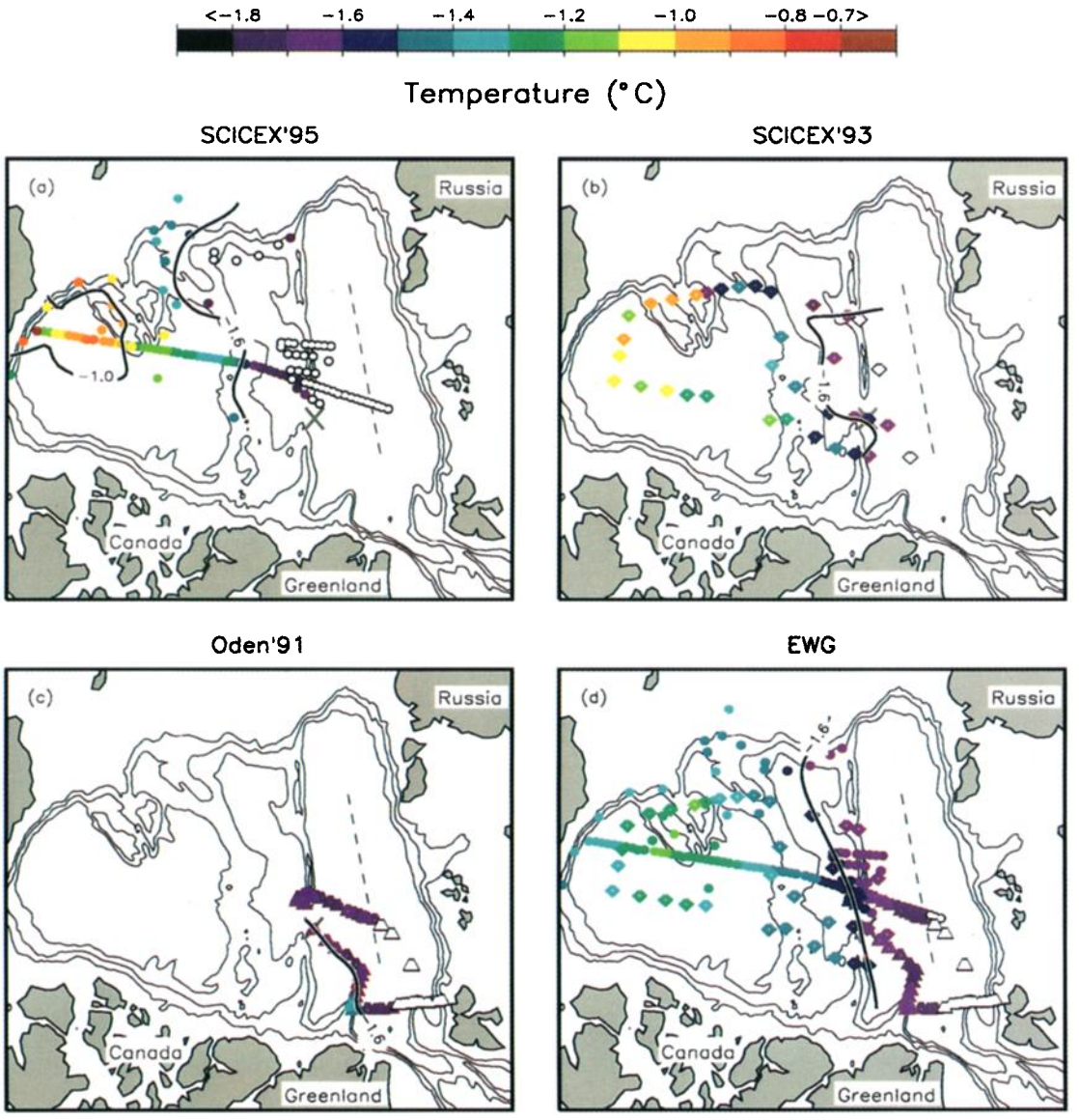

Plate 5. Same as Plate 3, but for the maximum temperature in each profile for salinities less than 33. This serves as a tracer for the slightly warm and relatively fresh Bering Sea Water (BSW). Stations with no salinities fresher than 33 are left as open circles. In Plate 5a, note the front at the Alpha-Mendeleyev Ridge. Temperatures near or at the freezing point probably do not represent true BSW, as discussed in the text.

0.1 N m^{-2} over a model simulation time of 20 days. The final state at day 20 is plotted in Plate 7. Spatial noise in the flux field derives from details of temperature and density stratification in each (somewhat noisy) profile. The main point is that heat fluxes up to about 2 W m^{-2} are generated over the Lomonosov and Nansen-Gakkel Ridges. These are significant values, especially since the usual expectation is that winter heat fluxes are nil in the Arctic Ocean interior [*Maykut and McPhee*, 1995]. Sensitivity experiments with varying surface stresses were also performed. A surface stress of 0.05 N m^{-2} yields negligible heat fluxes throughout the Arctic, while a surface stress of 0.15 N m^{-2} creates surface heat fluxes greater than 1.0 W m^{-2} in most of the Amundsen Basin and over the Lomonosov Ridge, with peak values of about 3.5 W m^{-2}.

Using an analytical model, *Rudels et al.* [1996] also estimated the amount of heat that might mix to the surface from the AW in the absence of a CHL. Their calculation yielded a value of 1.26 W m^{-2}, similar to maximum values in Plate 7. These winter fluxes are about an order of magnitude smaller than those estimated for summer 1975 in the Beaufort Sea by *Maykut and McPhee* [1995], which were generally several tens of watts per square meter. However, summer in the high Arctic is relatively short; *Maykut and McPhee* [1995] estimated that the annual average flux generated by summer heating was only 3.5–5.1 W m^{-2}. Assuming a 9 month winter season, annual average heat fluxes from the process modeled in Plate 7 would be as high as 1.5 W m^{-2}, or 30–40% of the annual average fluxes estimated by *Maykut and McPhee* [1995].

Thus our results predict a 30–40% increase in the annual average upward heat flux to the base of Arctic sea ice during 1995 in much of the Eurasian Basin and especially over the Lomonosov Ridge (to the extent that these winter and summer estimates are representative of the Arctic Ocean). Smaller, although significant heat fluxes are also apparent from Plate 7 in the Canada Basin as BSW is mixed to the surface, a signature of the "cool halocline" in this region. The only major Arctic Ocean basin in which such heat fluxes are nil is the Makarov Basin. If the presence of a CHL is defined

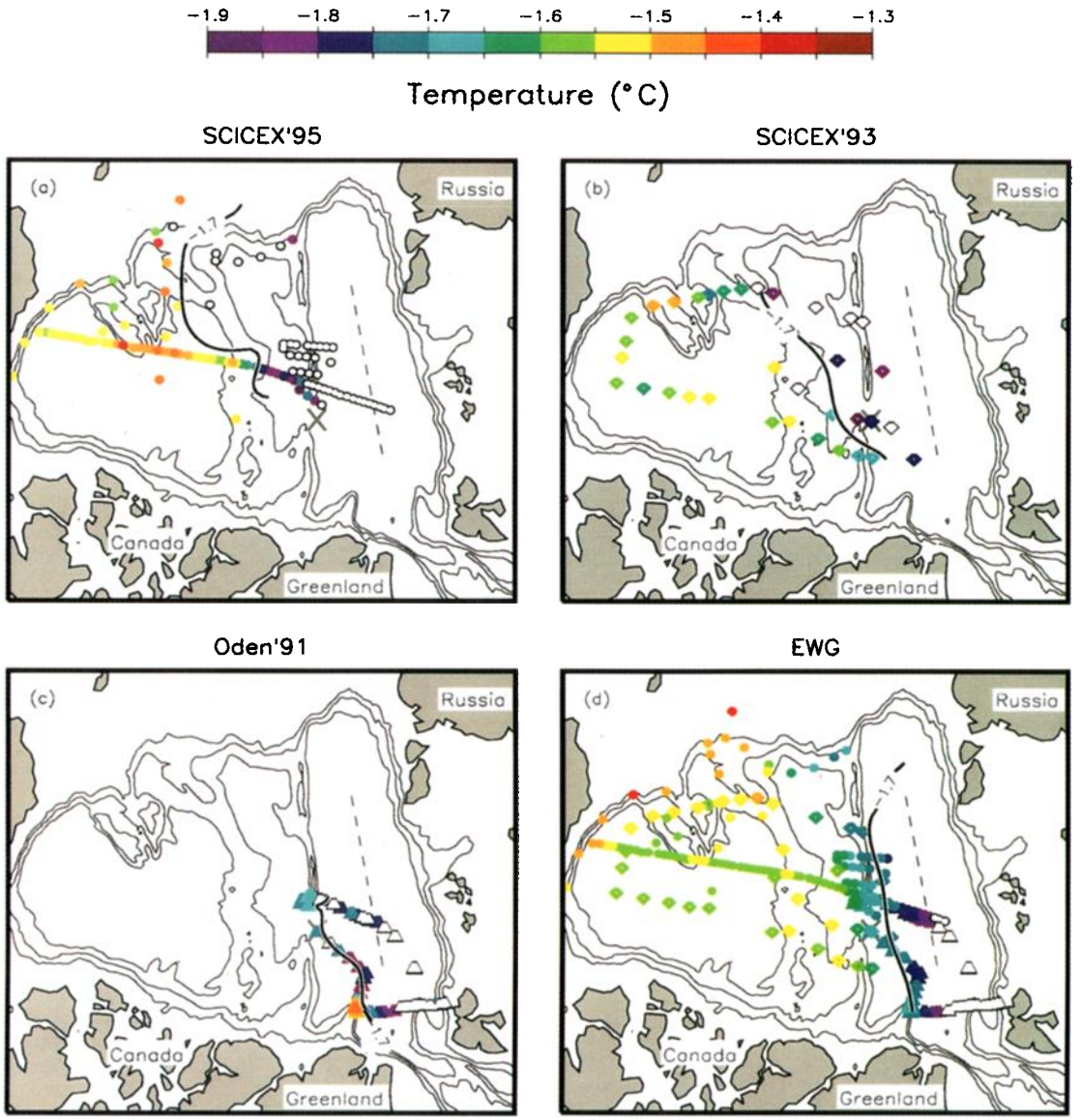

Plate 6. Same as Plate 3 but for the mean temperature in the layer containing salinities in the range $33.0 < S < 33.1$. This serves a tracer for Upper Halocline Water (UHW), which is centered at this salinity. As in Plate 5, open shapes denote stations where the salinity criterion was not met, while near-freezing temperatures probably do not represent true UHW (discussed in the text). Note the difference in temperature scales between this plate and Plate 5.

by the absence of upward oceanic heat flux during winter, then the Makarov was the only deep basin of the Arctic Ocean with a CHL during SCICEX'95.

What will be the effect of enhanced heat flux during winter on the sea ice mass balance? The answer is difficult to determine accurately without a full dynamic-thermodynamic model calculation, which is beyond the scope of this paper. Complex feedback mechanisms (such as between winter convection, heat flux, and ice growth) can influence the result [e.g., *Roach et al.*, 1993]. Generally, we expect that enhanced upward heat fluxes will lead to a reduction in winter ice growth. An upper bound can be provided by equating the ocean heat flux increase ΔF_w to a decrease in the freezing rate $\Delta \dot{h}$ (i.e., assuming no change in heat conduction up through the sea ice). In this case, $\Delta \dot{h} = -\Delta F_w / \rho L$, where $\rho = 910$ kg m^{-3} is the density of sea ice and $L = 3 \times 10^5$ J kg^{-1} is the latent heat of fusion for sea ice. For ΔF_w values of {0.5, 1.0, and 3.0} W m^{-2} we obtain $\Delta \dot{h}$ values of {−6, −12, and −35} cm yr^{-1}. These could represent a significant reduction in net winter ice growth in the interior of the Arctic Ocean, which has been estimated at 30–90 cm yr^{-1} [*Untersteiner*, 1961; *Maykut*, 1982; *Thomas et al.*, 1996]. Also, an increase of 1.5 W m^{-2} above the canonical value of 2 W m^{-2} used by *Maykut and Untersteiner* [1971] thins the equilibrium thickness of multiyear ice by about 2/3; i.e., a reduction from 3 to ~2 m.

6. A Possible Cause

The upper layers of the mid-Eurasian Basin are saltier than at any time since 1950 (Plate 1). We have speculated that this is due to a shift in the region influenced by western Siberian river runoff.

That is, we suggest that the inflow of such waters from the Kara and Laptev Seas has shifted from the Amundsen Basin to the Makarov Basin. The question then is what has caused this shift of the "injection point" of fresh shelf water into the deep basins during the 1990s.

Since we are dealing with fresh surface waters, the most likely explanation for these changes is a shift in the wind and resulting sea ice motion patterns. Figure 7 shows the annual mean fields of surface pressure and ice motion as computed from the International Buoy Program (I. Rigor, University of Washington, personal communication, 1997) for the years 1979–1987 (Figure 7a) and 1988–1996 (Figure 7b). The surface pressure pattern in both cases is to first order a dipole, with the Beaufort High pressure cell centered within the Canada Basin and the Eurasian Low pressure cell dominating the Eurasian sector of the Arctic Ocean. The ice motion pattern generally shows an anticyclonic circulation within the Canada Basin (in response to the Beaufort High) and a Transpolar Drift Stream that draws sea ice from Siberia and out through Fram Strait.

A recent paper by *Walsh et al.* [1996] demonstrated how the strength of the Beaufort High has weakened and moved eastward since the late 1980s. Figure 7 shows that this has been accompanied by an increase in the strength and extent of the Eurasian Low during this time. (For example, isobars between 1008 mb and 1014 mb have intruded much farther into the Arctic Ocean in the 1990s relative to the 1980s; further, more area is covered by cyclonically oriented isobars.) The result is a noticeable change in the main axis of the Transpolar Drift Stream, wherein this axis has shifted from the Eurasian sector to the Canadian sector. We mark this in Figure 7 by the location of the zero contour of the sea ice vorticity field (vertical component).

The Eurasian Low pressure cell has therefore extended farther into the Arctic Basin during the 1990s than in previous years. What effect might this have on the site where fresh riverine shelf waters might be injected into the deeper basins? We here propose the following scenario. Before the late 1980s, fresh surface waters from the Kara and Laptev Seas were carried either directly out into the Eurasian Basin via the Transpolar Drift Stream or carried quickly offshore to the right of the main drift via Ekman transport. During the 1990s, however, the Transpolar Drift Stream axis shifted significantly toward Canada, leaving in its wake a cyclonic circulation cell in the Laptev Sea (Figure 7b). The result should be transport either along the shelf with the ice motion or onto the shelf with the Ekman transport. Either way, we expect that riverine shelf water was carried much farther eastward during the 1990s relative to previous years. The result should be that such water eventually flows out into the deep basins at a point much farther east. We propose that this explains the retreat of fresh surface waters (and therefore a CHL) from the Amundsen Basin into the Makarov Basin.

Our hypothesis is supported by very recent ice drift simulations in this area (S. Pfirman, Barnard College, personal communication, 1997) as well as oceanic chemical tracer studies (K. Falkner, Oregon State University, personal communication, 1997). An alternate explanation of Eurasian Basin salinification might be proposed, however. It might simply be that river runoff into the Kara and Laptev Seas (and its export into the deep basins) has decreased during the 1990s. Unfortunately, Russian river runoff data from the 1990s are not available. We expect that time series of moisture flux convergence over the various river basins might provide a meaningful proxy.

Finally, we note that runoff is a highly seasonal phenomenon in the Arctic, since river ice forms during winter and essentially cuts off the transport. Thus one might argue that Figure 7 should only show data from summer and/or fall. However, we are not concerned here with the details of shelf processes and mixing. Studies

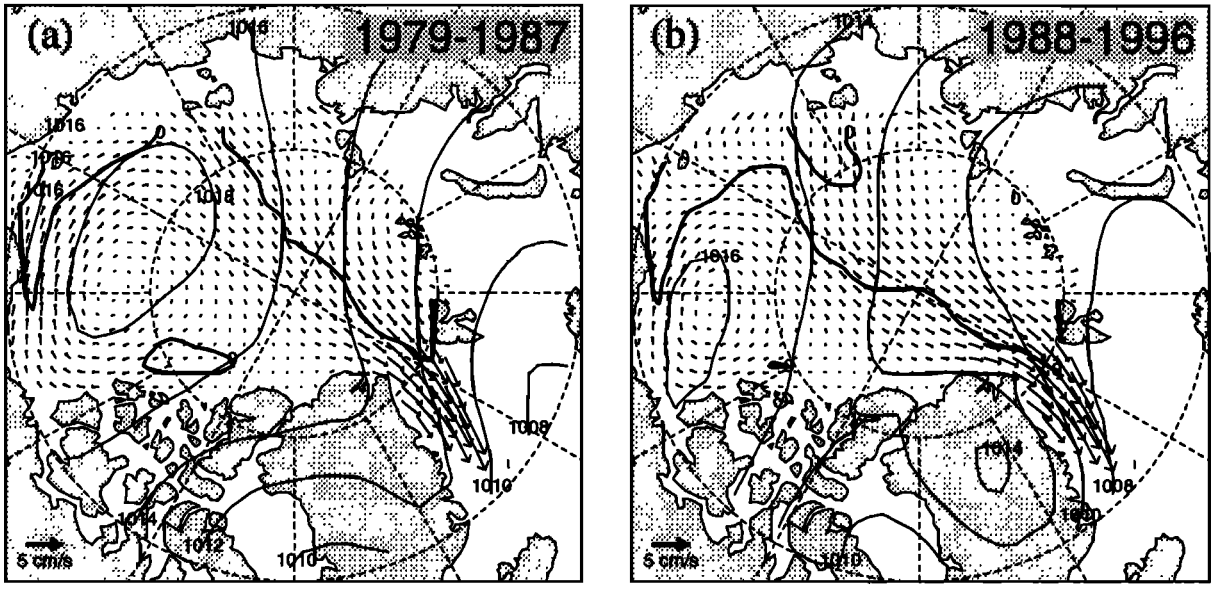

Figure 7. Average fields for the years (a) 1979–1987 and (b) 1988–1996 from the International Buoy Program (I. Rigor, University of Washington, personal communication, 1997). The vectors show the average sea ice motion, the thin contour lines show the average surface air pressure, and the heavy sold lines show the zero contour of the vertical component of the curl of the ice motion field. The latter traces the axis of the Transpolar Drift Stream, which separates the anticyclonic Beaufort Gyre from the generally cyclonic motion in the Eurasian Basin. A shift in this axis occurred in the late 1980s, which we speculate led to an eastward shift in the location where fresh shelf waters from the Kara and Laptev Seas are injected into the Arctic Ocean interior.

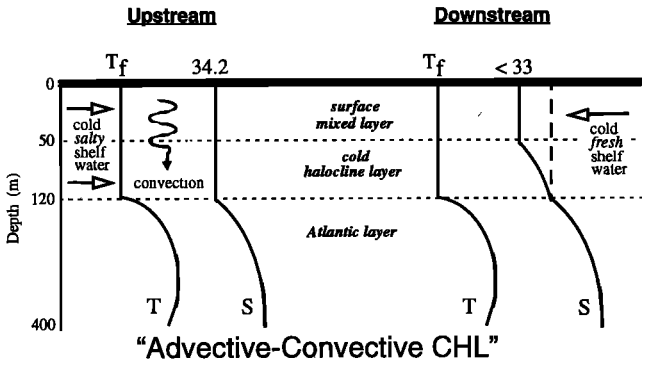

Figure 8. A schematic illustration of our view of cold halocline layer formation. The layer between 50 and 120 m depth in the Nansen Basin contains Lower Halocline Water, formed by a variety of processes in winter. These are advective (intrusions of cold, salty waters from the shelves) and convective (winter convection in the deep basin). Downstream from these LHW sources (somewhere near the Kara and Laptev Seas), relatively fresh shelf waters are injected into the surface and near-surface layers, resulting in a year-round fresh surface layer and the formation of a cold halocline layer.

have shown a residence time of about 3 years in these shelf regions [*Schlosser et al.*, 1994; *Pavlov and Pfirman*, 1995]; further, these shelf regions remain quite fresh even through the winter season (except perhaps at localized polynyas where ice forms). Thus the annual average data serve our purposes.

7. Comments on CHL Formation

In Figure 2a we show the usual way that CHL is supposed to form, by an advective interleaving of cold salty shelf waters into the deep basins. Figure 2b shows a new way, proposed by *Rudels et al.* [1996], that involves mixed layer convection and then interleaving of cold fresh shelf waters. A possible conflict then arises: Are shelf waters salty or fresh? One might answer that they are highly variable on a seasonal basis; that is, they are salty in winter and fresh in summer. But this is not quite true. The Siberian shelves eastward of the Kara Sea are all quite fresh even throughout winter, a fact noted by *Aagaard et al.* [1981] and confirmed by the climatologies [e.g., *EWG*, 1997]. The only salty (i.e., $S > 33$) shelf sea in the eastern longitudes of the Arctic Ocean is the Barents Sea, which led *Aagaard et al.* [1981] to speculate that this would be the most likely source of CHL formation via the mechanism shown in Figure 2a. A caveat is that salty water might form in the long polynyas along the boundary between fast ice and pack ice that lies

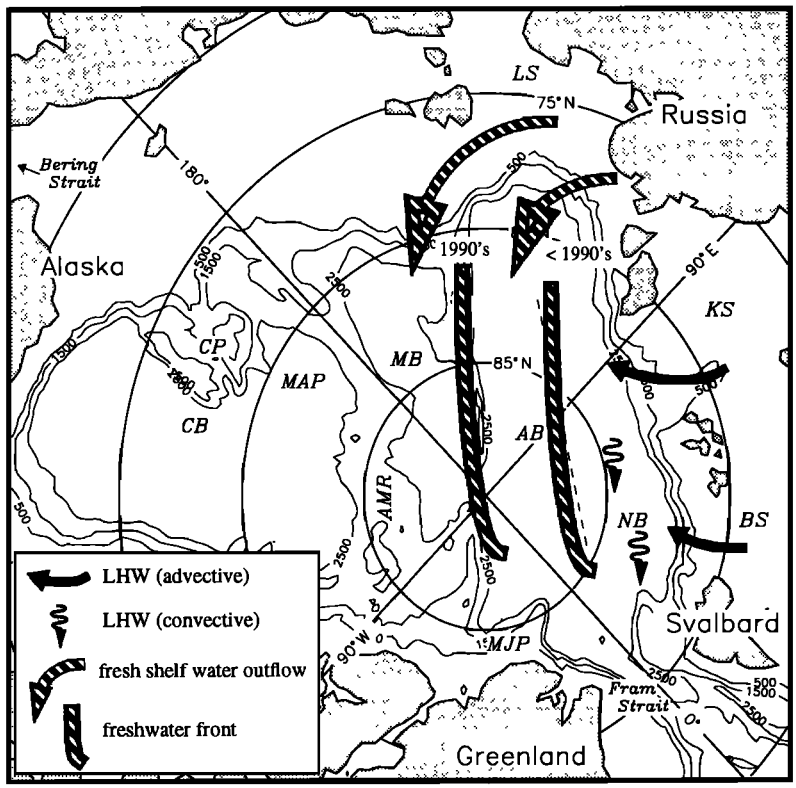

Figure 9. A schematic map of our view of cold halocline layer formation and retreat. Lower Halocline Water (LHW, solid arrows) forms in the western and central Nansen Basin by a combination of advective (curved arrows) and convective (wavy arrows) processes, creating a deep winter mixed layer at freezing temperatures and a salinity of about 34.0–34.2. Injection of fresher shelf waters (striped arrows) into the Eurasian Basin occurs somewhere east of 90°E longitude. The result is a year-round freshwater "cap" that creates a true cold halocline layer. The position of this injection point and the associated front that defines the boundary of fresh shelf-derived waters (striped curves) has shifted over the course of the 1990s.

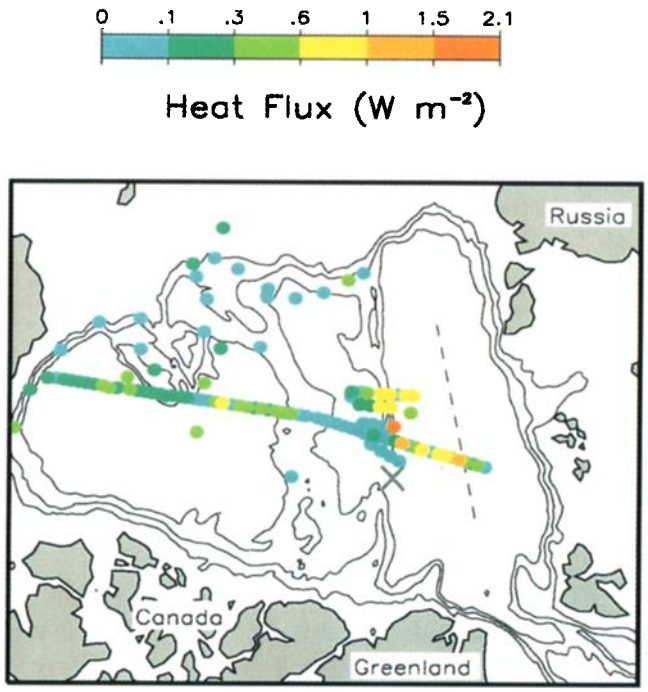

Plate 7. The surface heat flux during SCICEX'95 as generated from a one-dimensional mixing model. Observed temperature and salinity profiles were used as initial conditions, while the surface mixing over a 20 day simulation was fixed at 0.1 N m^{-2}. Maximum heat fluxes were obtained in the Eurasian Basin and over the Lomonosov Ridge, where the cold halocline layer has vanished.

far offshore in the Laptev Sea. Recent analysis indicates that this process is too weak to produce waters salty enough for CHL formation (D. Detleff, GEOMAR Research Center for Marine Geosciences, Kiel, Germany, personal communication, 1997). Generally speaking, then, we can say that some shelves are salty and some are (relatively) fresh.

The advective CHL formation mechanisms proposed by *Aagaard et al.* [1981] and *Steele et al.* [1995] therefore should produce interleaving of cold salty waters from somewhere near the Barents Sea. But this presents a problem. Figure 2a shows a proposed mechanism whereby these waters should be interleaving, in winter, into an upstream condition with a very fresh surface layer. However, this layer simply does not exist offshore of the Barents Sea continental shelf. Rather, Plate 1 and the full *EWG* [1997] climatology (not shown) indicate that most of the Nansen Basin during winter is quite salty (i.e., $S > 34$) even at the surface. This is also confirmed by the winter hydrographic data collected in this region by *Perkin and Lewis* [1984]. As discussed in section 4.2, such high salinities are the result of winter convection in the absence of a riverine influence.

Thus, during winter, northward flowing cold, salty waters from the Barents Sea are confronted with a deep Arctic Ocean mixed layer of similarly high salinity. Therefore interleaving could occur anywhere within this mixed layer of about 100–150 m thickness. The only time that interleaving would be mostly confined below a fresh surface layer is when such a thing exists in the western Nansen Basin, i.e., during summer and early fall when a fresh surface ice melt layer is extant.

It is not our intention here to make a definitive statement about the way that the CHL forms. However, we do question the role that the purely "advective" mechanism in Figure 2a plays, and we propose a new view of CHL formation in the eastern Arctic Ocean, shown in Figures 8 and 9. Figure 8 is simply modified from Figure 2b by including the advection of cold salty shelf waters into the salty deep winter mixed layer of the Nansen Basin, upstream from the point where cold fresh shelf waters are injected into the interior. Figure 9 shows these processes in plan view and includes the presumed shift in the region influenced by fresh shelf waters that occurred sometime in the late 1980s.

8. Conclusions

The mid-Eurasian Basin has undergone a remarkable salinification of its surface waters during the 1990s, and is now saltier than at any time since 1950, the first year for which climatological data are available (Figures 4 and 5 and Plate 1). The result is a retreat of the cold halocline layer from the Eurasian Basin into the Makarov Basin. We could just as well call this a "reduction" in the extent of year-round CHL influence, where before the 1990s it covered the Makarov and Amundsen Basins and during the 1990s it was reduced to cover only the Makarov Basin. A simple model calculation indicates that in the Eurasian Basin, significant heat fluxes may be rising from the deep (but rapidly shoaling) Atlantic Water layer toward the surface (Plate 7).

We suspect that these changes are forced by the intrusion of the Eurasian Low pressure cell into the Arctic Basin during the 1990s (Figure 7) and an accompanying shift in ice drift and upper ocean circulation patterns. We further note that the strengthening of the annual average Eurasian Low is in one sense a reflection of increased storm activity (i.e., low-pressure phenomena) in this region. This should lead to enhanced surface mixing, so that our estimates of upward heat flux in Plate 7 might in fact be somewhat too low.

Recent icebreaker cruises have encountered very light ice conditions in the Eurasian Basin (R. Muench, Earth and Space Research,

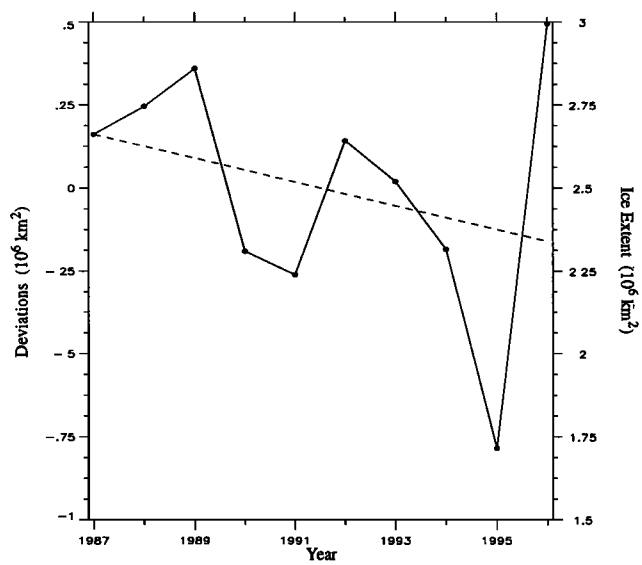

Figure 10. September mean ice extent in the Eurasian Basin for 1987–1996 using data from the special sensor microwave/imager (SSM/I). The solid line with dots shows the area contained by the 15% sea ice concentration contour from 0°–150°E longitude. The dashed line shows the least squares fit, which has a slope of -0.0285×10^6 km^2 yr^{-1}.

personal communication, 1997). This, of course, could be the result of any number of thermodynamic and/or dynamic processes. A thorough analysis of sea ice conditions in the 1990s is beyond the scope of this paper. We have, however, examined satellite passive microwave imagery from the special sensor microwave/imager (SSM/I). As a measure of minimum sea ice extent, we plotted in Figure 10 the September average 15% sea ice concentration contour from 0°–150°E longitude from each year of 1987–1996. While there is large interannual variability, the total ice extent in this sector of the Arctic exhibits a negative least squares slope of -0.0285×10^6 km^2 yr^{-1}. This is close to the slope obtained by *Cavalieri et al.* [1997] for the total Arctic ice extent from 1978–1996.

So will these changes in the upper Arctic Ocean continue or will they swing back toward more "usual" conditions? We cannot say. Recent modeling work indicates the presence of roughly decadal swings in the wind forcing in the Arctic, from conditions dominated by anticyclonic to cyclonic and back again [*Proshutinsky and Johnson*, 1997]. Yet much of our data (e.g., winter surface salinities in the Eurasian Basin) lie outside the historical 40 year climatological range, indicating that a longer timescale transition occurred some time in the late 1980s. Only continued monitoring of the Arctic Ocean can provide the answers to these questions.

Acknowledgments. This study would not have happened without the encouragement and advice of James Morison, who also provided SCICEX'93 data. G. Bjork provided *Oden*'91 data. Thanks to M. S. Moustafa, R. Keenan, and P. Mikhalevsky for their efforts in SCICEX'95 data calibration and organization and to J. Annis and T. J. Saunders for manipulating and graphing it with speed and good humor. We thank I. Rigor for graciously making the ice motion and surface pressure data available. The comments and suggestions of K. Aagaard, S. Martin, D. Rothrock, and the anonymous reviewers were much appreciated. This work was supported by the High Latitude Program at the Office of Naval Research, grants N00014-95-1-0437 (M. S.) and N00014-95-1-0479 (T. B.). Additional support for M. Steele was provided by an EOS interdisciplinary investigation, Polar Exchange at the Sea Surface (POLES), NASA grants NAGW-2407 and NAG5-4375.

References

Aagaard, K., L. K. Coachman, and E. Carmack, On the halocline of the Arctic Ocean, *Deep Sea Res., Part A, 28*, 529–545, 1981.

Anderson, L. G., G. Björk, O. Holby, E. P. Jones, G. Kattner, K. P. Koltermann, B. Liljeblad, R. Lindegren, B. Rudels, and J. Swift, Water masses and circulation in the Eurasian Basin: Results from the *Oden* 91 expedition, *J. Geophys. Res., 99*, 3273–3283, 1994.

Bauch, D., P. Schlosser, and R. G. Fairbanks, Freshwater balance and the sources of deep and bottom waters in the Arctic Ocean inferred from the distribution of $H_2{}^{18}O$, *Prog. Oceanogr., 35*, 53–80, 1995.

Cavalieri, D. J., P. Gloersen, C. L. Parkinson, J. C. Comiso, and H. J. Zwally, Observed hemispheric asymmetry in global sea ice changes, *Science, 278*, 1104–1106, 1997.

Coachman, L. K., and C. A. Barnes, The contribution of Bering Sea water to the Arctic Ocean, *Arctic, 14*, 147–161, 1961.

Colony, R., and A. S. Thorndike, An estimate of the mean field of Arctic sea ice motion, *J. Geophys. Res., 89*, 10,623–10,629, 1984.

D'Asaro, E. A., and J. H. Morison, Internal waves and mixing in the Arctic Ocean, *Deep Sea Res., Part A, 39*, suppl., S459–S484, 1992.

Environmental Working Group (EWG), *Joint U.S.–Russian Atlas of the Arctic Ocean* [CM-ROM], Natl. Snow and Ice Data Cent., Boulder, Colo., 1997.

Jones, E. P., and L. G. Anderson, On the origin of the chemical properties of the Arctic Ocean halocline, *J. Geophys. Res., 91*, 10,759–10,767, 1986.

Martin, S., and D. J. Cavalieri, Contributions of the Siberian shelf polynyas to the Arctic Ocean intermediate and deep water, *J. Geophys. Res., 94*, 12,725–12,738, 1989.

Maykut, G. A., Large-scale heat exchange and ice production in the central Arctic, *J. Geophys. Res., 87*, 7971–7984, 1982.

Maykut, G. A., and M. G. McPhee, Solar heating of the Arctic mixed layer, *J. Geophys. Res., 100*, 24,691–24,703, 1995.

Maykut, G. A., and N. Untersteiner, Some results from a time-dependent, thermodynamic model of sea ice, *J. Geophys. Res., 76*, 1550–1575, 1971.

McLaughlin, F. A., E. C. Carmack, R. W. Macdonald, and J. K. B. Bishop, Physical and geochemical properties across the Atlantic/Pacific water mass front in the southern Canadian Basin, *J. Geophys. Res., 101*, 1183–1197, 1996.

McPhee, M. G., Turbulent heat flux in the upper ocean under sea ice, *J. Geophys. Res., 97*, 5365–5379, 1992.

Mellor, G. L., and T. Yamada, Development of a turbulence closure model for geophysical fluid problems, *Rev. Geophys. Space Phys., 20*, 851–875, 1982.

Mellor, G. L., M. G. McPhee, and M. Steele, Ice-seawater turbulent boundary layer interaction with melting or freezing, *J. Phys. Oceanogr., 16*, 1829–1846, 1986.

Moore, R. M., M. G. Lowings, and F. C. Tan, Geochemical profiles in the central Arctic Ocean: Their relation to freezing and shallow circulation, *J. Geophys. Res., 88*, 2667–2674, 1983.

Morison, J. H., and J. D. Smith, Seasonal variations in the upper Arctic Ocean as observed at T3, *Geophys. Res. Lett., 8*, 753–756, 1981.

Morison, J. H., M. Steele, and R. Andersen, Hydrography of the upper Arctic Ocean measured from the nuclear submarine USS *Pargo*, *Deep Sea Res., Part I*, in press, 1998.

Newton, J. L., and B. J. Sotirin, Boundary undercurrent and water mass changes in the Lincoln Sea, *J. Geophys. Res., 102*, 3393–3403, 1997.

Padman, L., and T. M. Dillon, Turbulent mixing near the Yermak Plateau during the Coordinated Eastern Arctic Experiment, *J. Geophys. Res., 96*, 4769–4782, 1991.

Pavlov, V. K., and S. L. Pfirman, Hydrographic structure and variability of the Kara Sea: Implications for pollutant distribution, *Deep Sea Res., Part II, 42*, 1369–1390, 1995.

Perkin, R. G., and E. L. Lewis, Mixing in the West Spitsbergen Current, *J. Phys. Oceanogr., 14*, 1315–1325, 1984.

Proshutinsky, A. Y., and M. A. Johnson, Two circulation regimes of the wind-driven Arctic Ocean, *J. Geophys. Res., 102*, 12,493–12,514, 1997.

Roach, A. T., K. Aagaard, and F. Carsey, Coupled ice-ocean variability in the Greenland Sea, *Atmos. Ocean, 31*, 319–337, 1993.

Rudels, B., E. P. Jones, L. G. Anderson, and G. Kattner, On the intermediate depth waters of the Arctic Ocean, in *The Polar Oceans and Their Role in Shaping the Global Environment: The Nansen Centennial Volume, Geophys. Monogr. Ser.*, vol. 85, edited by O. M. Johannessen, R. D. Muench, and J. E. Overland, pp. 33–46, AGU, Washington, D. C., 1994.

Rudels, B., L. G. Anderson, and E. P. Jones, Formation and evolution of the surface mixed layer and halocline of the Arctic Ocean, *J. Geophys. Res., 101*, 8807–8821, 1996.

Schlosser, P., D. Grabitz, R. Fairbanks, and G. Bonisch, Arctic river-runoff: Mean residence time on the shelves and in the halocline, *Deep Sea Res., Part I, 41*, 1053–1068, 1994.

Steele, M., and J. H. Morison, Hydrography and vertical fluxes of heat and salt northeast of Svalbard in autumn, *J. Geophys. Res., 98*, 10,013–10,024, 1993.

Steele, M., G. L. Mellor, and M. G. McPhee, Role of the molecular sublayer in the melting or freezing of sea ice, *J. Phys. Oceanogr., 19*, 139–147, 1989.

Steele, M., J. H. Morison, and T. Curtin, Halocline water formation in the Barents Sea, *J. Geophys. Res., 100*, 881–894, 1995.

Steele, M., D. Thomas, D. Rothrock, and S. Martin, A simple model study of the Arctic Ocean freshwater balance, 1979–1985, *J. Geophys. Res., 101*, 20,833–20,848, 1996.

Swift, J. H., E. P. Jones, K. Aagaard, E. C. Carmack, M. Hingston, R. W. MacDonald, F. A. McLaughlin, and R. G. Perkin, Waters of the Makarov and Canada Basins, *Deep Sea Res., Part II*, in press, 1998.

Thomas, D., S. Martin, D. Rothrock, and M. Steele, Assimilating satellite concentration data into an Arctic sea ice mass balance model, 1979–1985, *J. Geophys. Res., 101*, 20,849–20,868, 1996.

Untersteiner, N., On the mass and heat budget of Arctic sea ice, *Arch. Meteorol. Geophys. Bioklimatol., Ser. A, 12*, 151–182, 1961.

Untersteiner, N., On the ice and heat balance in Fram Strait, *J. Geophys. Res., 93*, 527–531, 1988.

Walsh, J. E., W. L. Chapman, and T. Shy, Recent decrease of sea level pressure in the central Arctic, *J. Clim., 9*, 480–486, 1996.

Zhang, J., W. Hibler, M. Steele, and D. Rothrock, Arctic ice-ocean modeling with and without climate restoring, *J. Phys. Oceanogr., 28*, 191–217, 1998.

T. Boyd, College of Oceanic and Atmospheric Sciences, Oregon State University, Corvallis, OR 97330.

M. Steele, Polar Science Center, Applied Physics Laboratory, College of Ocean and Fishery Sciences, University of Washington, 1013 NE 40th Street, Seattle, WA 98105-6698. (e-mail: mas@ apl.washington.edu)

(Received October 6, 1997; revised January 11, 1998; accepted February 11, 1998.)